Journal of Organometallic Chemistry 854 (2018) 38–48

Contents lists available at ScienceDirect

Journal of Organometallic Chemistry

journal homepage: www.elsevier.com/locate/jorganchem

Non-rigid coordination behavior of the ambidentate phosphinoyldithioformate ligands, $[S_2CP(O)R_2]^-$, (R = Ph, CH_2Ph) in organometallic Lead(IV) and Mercury(II) compounds

Sigurjon N. Ólafsson, Águst Kvaran, Sigridur Jonsdottir, Sigridur G. Suman*

Science Institute, University of Iceland, Dunhagi 3, 107 Reykjavik, Iceland

ARTICLE INFO

Article history:
Received 19 May 2017
Received in revised form
28 October 2017
Accepted 1 November 2017
Available online 5 November 2017

Keywords:
Pb(IV)
Hg(II)
^{31}P NMR
Non-rigid
Ambidentate
Phosphinoyl
Dithioformate

ABSTRACT

A series of phosphinoyldithioformate compounds were synthesized from metathesis reactions of K $[R_2P(O)CS_2]$, and R'_nPbCl_{4-n} and R'HgCl. The compounds isolated were characterized using infrared, UV and multinuclear NMR (^1H, ^{13}C, and ^{31}P) spectroscopy. Structural diversity of these compounds is revealed through analysis of the infrared and NMR spectroscopy, where variable temperature ^{31}P NMR spectroscopy data of **6** reveals non-rigid coordination behavior and an equilibrium of *aniso* bonded S,S 4-membered ring, and S,O bonded 5-membered ring bonding modes in $[MeHg\{S_2CP(O)(Ph)_2\}]$, (**6**–**6′**). The crystal structure of **6′** shows the mercury atom in a T-shape geometry with S,O-bidentate coordinated ligand although room temperature NMR indicated the coordination to the mercury in **6** is non rigid in solution. Variable temperature ^{31}P NMR spectroscopy yielded an average value of $\Delta G^{\#}_{\mathbf{6}\text{-}\mathbf{6'}} = 45.7 \pm 1.7$ kJ mol^{-1} for the temperature range of 190 K–283 K. The crystal structure of $[Ph_2Pb\{S_2CP(O)(Ph)_2\}_2(H_2O)]$, **1**, reveals the lead atom in an unusual seven coordinate geometry with two S,O-bidentate coordinated ligands and axial phenyl groups. The seventh ligand is a water molecule bonded to lead forming a pentagonal plane.

1. Introduction

Substituted dithioformates XCS_2^- (X = R, NR_2, OR, SR) are well known ligands for most metal ions and have been reviewed several times [1,2]. The structural diversity of organometallic compounds of lead(IV) with ambidentate ligands with substituted dithioformates and related dichalogen donor atom ligands has been reviewed recently [3]. Ambidentate ligands of phosphinoyldithioformates with a mixture of hard/soft donors like sulfur and oxygen have received considerable attention, revealing a pattern for preferred geometry and coordination number for group 14 compounds [4–6].

A dichalcogenimidodiphoshinato anionic ligand, $[(XPR_2)(YPR_2)N]^-$ shown in Scheme 1(a–c) (X = O, S, Se; Y = O, S, Se; R = Me or Ph) and its lead(IV) compound structures have been investigated extensively [1,7,8]. If reacted in appropriate stoichiometry they form tetrahedral complexes, forming bidentate, six membered, chelate structures. Small changes of the donor atom from sulfur to selenium were reported sufficiently important to induce solid-state intramolecular interactions in dithiophosphinato ligands [9]. Similarly, trigonal bipyramidal structures are obtained with the ligands in Scheme 1(d and e) with donor atoms as either S,S, or O,O, and R groups as either methyl or phenyl [10]. In complexes with the formula R_2PbL_2, where L (Scheme 1 d) and e)) is a bidentate donor, octahedral structures prevail, and the aryl groups were found *trans* to each other [11].

Compounds of dithiophosphinato ligands, $M[R_2PS_2]$ (M = Na, K) are known to exhibit ambidentate coordination geometries of the dithiogroup to Pb to form either monodentate tetrahedral complexes [12] (R = OEt; Scheme 1(d)), or four membered rings with bidentate dithiogroup in distorted octahedral geometry (R = Ph, OCH_2Ph or OBz), with the shorter S-Pb(IV) bonds as *trans* to the π-interactions leading to an asymmetric coordination [13]. Polymeric structures were found for methyl ligands (Scheme 1(d)) exhibiting trigonal bipyramidal geometry around the lead atom [14]. Compounds with $R_2PO_2^-$ (R = Ph, Me, Scheme 1(e)) also exhibit known dimeric structures with lead centers in an octahedral geometry, and with oxygen atom doubly bridging to the lead atoms [15].

The possible coordination modes of $[R_2P(O)CS_2]^-$ are shown in

* Corresponding author.
E-mail address: sgsuman@hi.is (S.G. Suman).

https://doi.org/10.1016/j.jorganchem.2017.11.002
0022-328X/

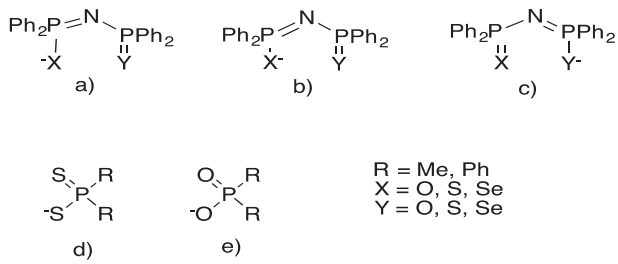

Scheme 1. Bidentate phosphinato ligands.

Scheme 2. These ligands may be monodentate (Scheme 2(1)) with one sulfur donor, or the dithioformate may act as a bidentate donor (Scheme 2: (2) and (3)), or the oxygen atom on the phosphine may act as a second electron donor to the lead (Scheme 2: (4) and (5)). In the bidentate coordination modes the second sulfur or oxygen act either as an electron pair donors, or through an *aniso* Pb-X bond (X = S, O) by an intermolecular interaction. The coordination mode of L1 and L2 is expected to be influenced by the Lewis acid properties of the central atom and by the other ligands present in the compounds formed. Therefore, a soft Lewis acid such as Ag(I) is expected to show different bonding preference than a hard Ge(IV). In this context, unpublished results for the $[PPh_3)_2Ag(L)]$ complexes synthesized in our laboratory show *iso* S,S bidentate bonding mode with observed Ag-S bond distances as 2.658 Å and 2.716 Å in their crystal structures.

A series of di-aryl substituted, trigonal bipyramidal R_2PbXL (L = L1, or L2 in Scheme 3, X = halogen) compounds possessing one halogen and dithiophosphinoyl ligand was reported previously [16]. These compounds all behave as discrete molecules in the solid state and in solution. The preferred coordination geometry for the ligands L1 and L2 with aryl ligands is an S,O-bidentate coordination as shown in Scheme 2(4). As shown in Scheme 2, one dithioformate sulfur is always coordinated to the metal center [1]. We also synthesized and reported several alkyl tin(IV) compounds [17]. The tin(IV) alkyl substituted compounds show large variety in structural preferences, existing both as discrete molecules and polymers in the solid state. The coordination preference of the Sn(IV) compounds is predominantly S,O bidentate in the solid state with L1 and L2, and in compounds composed of only L1, or L2 and alkyl ligands the S,O coordination is maintained in solution. Compounds with mixed halogen and alkyl ligands and L1 or L2 showed dissociation of the oxygen donor in solution forming monodentate S coordinated L1 or L2. As a hard Lewis acid, Sn(IV) was expected to prefer coordination to the oxygen donor if possible. It was therefore of great interest to investigate the behavior of the similarly alkyl substituted compounds with an intermediate Lewis acid, such as

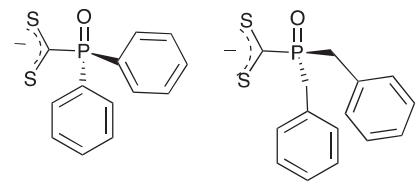

Scheme 3. Structures of ligands L1 (left) and L2 (right).

Pb(IV), and a soft Lewis acid, such as Hg(II), and the phosphinoyldithioformate ligands and confirm their solid and solution state structural preferences. Mercury is expected to show preferentially discrete molecular structures because of its propensity for low coordination number. Organometallic mercury(II) compounds show interesting solid state structures when coordinated to dithiocarbamate ligands where this propensity is displayed in *aniso* bidentate coordination of the dithiocarbamate and T shape geometry around the Hg(II) center [18]. The coordination geometry preference of Hg(II) is further displayed by steric effects where bulky ligands promote singly bonded dithiocarbamate coordination as well as preventing intermolecular interactions [19].

We present here our studies of organometallic lead(IV) and mercury(II) compounds with the ambidentate chelate anion $[R_2P(O)CS_2]^-$ (R = Ph (L1), and R = Bz (L2)). The synthesis and properties of compounds of the alkyl compounds with the general formula $[R_3Pb(L)]$, and Hg(II) compounds with the formula [RHg(L)] are reported. The solid state structures of the compounds were inferred using IR spectroscopy, and X-ray diffraction data was obtained for **1**, $[Ph_2Pb(L1)_2(H_2O)]$, and **6′**, [MeHg(L1)]. We previously reported a six coordinate analog of **1** [16]. The current structure shows an unexpected and unusual seven coordinate lead(IV) with pentagonal bipyramidal structure. The lead(IV) and mercury(II) both have NMR active isotopes allowing for multinuclear analysis of the solution structures of their compounds. Multinuclear NMR spectroscopic data of the compounds were analyzed to elucidate the coordination geometry of the compounds in solution. Alkyl mercury compound **6** exhibits non-rigid coordination properties where the solution and solid state structures are labeled **6** and **6′** respectively. The solid and solution state data of **6** and **6′** were elucidated employing infrared and NMR spectroscopy. Variable temperature ^{31}P NMR study of **6** confirms non-rigid coordination behavior of L1.

2. Results and discussion

2.1. Syntheses

Eight new organolead(IV) and organomercury(II) derivatives with phosphinoyldithioformate ligands were prepared using

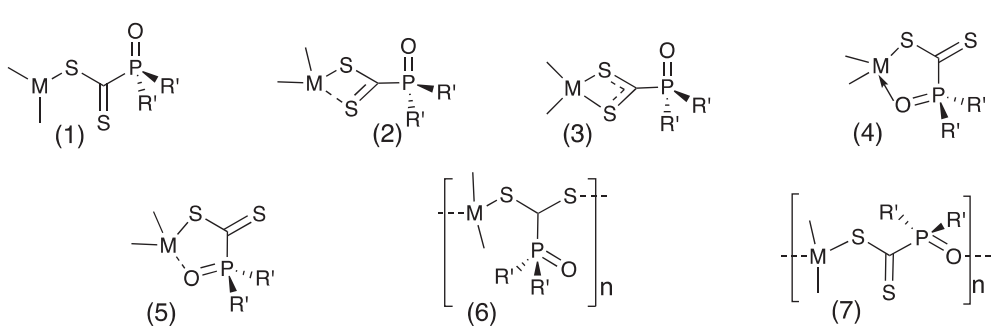

Scheme 2. Possible coordination modes of ligands L1 and L2, with Pb and Hg.

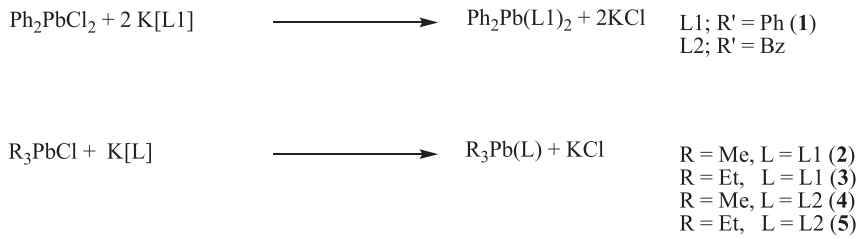

Scheme 4. Synthesis of lead compounds.

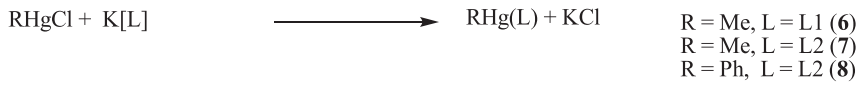

Scheme 5. Synthesis of mercury compounds.

Table 1
Physical and Analytical Data for all compounds.

Compound	Color	Yield (%)	M.p. (°C)	Analysis (%), C	Calc(found) H	δ^{31}P(ppm)[a] [^2J(M,P)] Hz
1 [$PbPh_2(L1)_2(H_2O)$]	purple	75	156–157	48.8 (48.9)	3.30 (3.45)	28.9 [90]
2 [$Me_3Pb(L1)$]	redbrown	77	107–108	36.3 (36.2)	3.62 (3.66)	18.6
3 [$Et_3Pb(L1)$]	orange	65	98–99	39.9 (39.2)	4.41 (4.32)	25.6
4 [$Me_3Pb(L2)$]	orange	84	130–131	38.8 (38.8)	4.16 (4.19)	37.3
5 [$Et_3PbEt_3(L2)$]	orange	75	130–131	42.1 (41.4)	4.87 (4.81)	38.7
6 [MeHg(L1)]	blue	59	98–99	34.1 (34.2)	2.66 (2.63)	27.2
7 [MeHg(L2)]	violet	62	106–108	36.9 (36.9)	3.29 (3.23)	41.6
8 [PhHg(L2)]	pink	73	165–167	43.3 (42.2)	3.28 (3.23)	41.1

[a] M = ^{207}Pb or ^{199}Hg.

stoichiometric amounts of the potassium salts of the ligands with the appropriate organolead or organomercury chloride reagents in acetone or dichloromethane according to Schemes 4 and 5.

All products are colored solids. Table 1 summarizes the physical properties of the compounds. The methyl substituted compounds **2** and **4** showed limited solubility in *non*-coordinating solvents, suggesting oligomerization or polymerization of the products according to (6) and (7) in Scheme 2. All other compounds were sufficiently soluble in chlorinated solvents for spectroscopic characterization. The compounds were characterized employing IR and multinuclear NMR spectroscopy (^{1}H, ^{13}C, ^{31}P) and the molecular structures of **1** and **6′** were determined by single crystal X-ray diffraction.

Stoichiometric reaction of Et_2PbCl_2 and 2 K[L2], in either acetone or methanol at 298 K or at 273 K, did not afford the expected 1:2 compound, $Et_2Pb[L2]_2$. Two products $Et_3Pb[L2]$ **5,** and $Pb[L2]_2$, were isolated and characterized. The thioester (L-R in Scheme 6) was identified by NMR, followed by *de novo* synthesis and characterization.[1] Our results suggest that fast redistribution and successive reductive elimination reaction takes place in solution as shown in Scheme 6. Similar redistribution reactions were discussed in a review of lead(IV) compounds with organometallic alkyl, and bidentate ligands with chalcogen donor atoms [20]. Reduced solubility of compounds **2** and **4,** who also possess organometallic alkyl ligands, may prevent the redistribution reaction. Similar compounds containing Sn(IV) with alkyl ligands by the formula $[SnR_2(L)_2]$ do not participate in a redistribution reaction [17]. Harder Lewis acids like Sn(IV) likely prevent the redistribution reaction because Sn(IV) only forms singly S-bonded compounds upon dissolution after isolation of S,O bonded species. Attempts to form Ge(IV) compounds with L1 or L2 resulted in isolation of white solids. Spectroscopic evaluation confirmed absence of the CS_2 moiety. These solids are currently under further study.

The stoichiometric reaction of methylmercury chloride with L1 or L2 yields compounds **6** and **7** respectively. Compound **8** is easily formed from PhHgCl and L2 ligand as a soluble discrete molecule. Attempted synthesis of [PhHg(L1)] gave a product that appeared to be the desired product judging from spectroscopic data, although we were not able to purify it or characterize properly.

2.2. Molecular structures of *1*, and *6*

Purple crystals of $[Ph_2Pb\{S_2CP(O)Ph_2\}_2(H_2O)]$, **1** suitable for X-ray diffraction were obtained by diffusion of Et_2O into a CH_2Cl_2 solution. The distorted pentagonal bipyramidal structure of **1** is shown in Fig. 1. The six coordinate structure of **1** was reported previously [16]. Selected bond distances and angles are listed in Table 2 and the crystallographic data is given in Supporting Information, Table S1.

The lead in $[Ph_2Pb(L1)_2(H_2O)]$, **1**, is coordinated in a distorted pentagonal bipyramidal (pbp) environment framed by two axial phenyl groups, two S,O-coordinating *aniso*-bidentate phosphinoyldithioformate ligands and one H_2O molecule. The P-C distances (2.170(1), 2.170(3) Å) are comparable to those (2.176, 2.215 Å) found in $[Ph_2Pb\{S_2P(OBz)_2\}_2]$ [10]. The C(1)-Pb-C(7) angle of 161.3(8)° is 10.0° wider than in the analogous octahedral compound [16], and the two *trans* Pb-C bonds are tilted towards the wider O(2)-Pb-O(1) angle.

[1] **Notes**(a) ^{31}P NMR of $[Pb(L2)_2]$ shows a singlet at δ = 39.7 ppm.(b) BzP(O)CS_2(Et): IR(KBr) $\tilde{\nu}$(cm^{-1}): 1201(P=O), 1088(CS_2), 891(CS_2). ^{31}P NMR($CDCl_3$), δ(ppm): 42.74 (^1J(^{31}P-$^{13}C_{ipso}$) 65.40 Hz, ^3J(^{31}P-$^{13}C_{Et}$) 2.0 Hz), ^{13}C NMR($CDCl_3$) δ: 238.3 ppm, (^1J(^{31}P-$^{13}C_{CS2}$) 64.47 Hz).

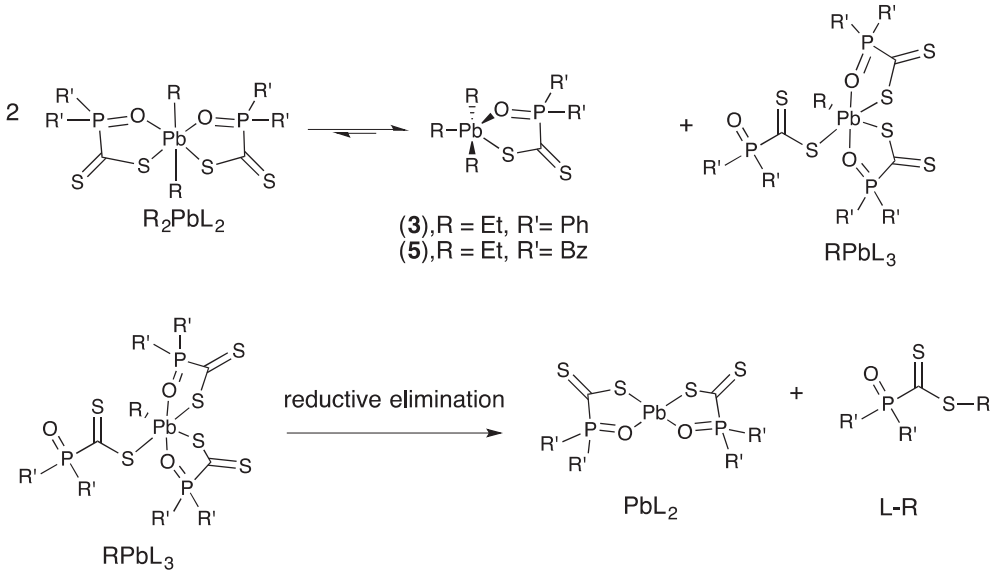

Scheme 6. Redistribution reaction of Et2PbL.

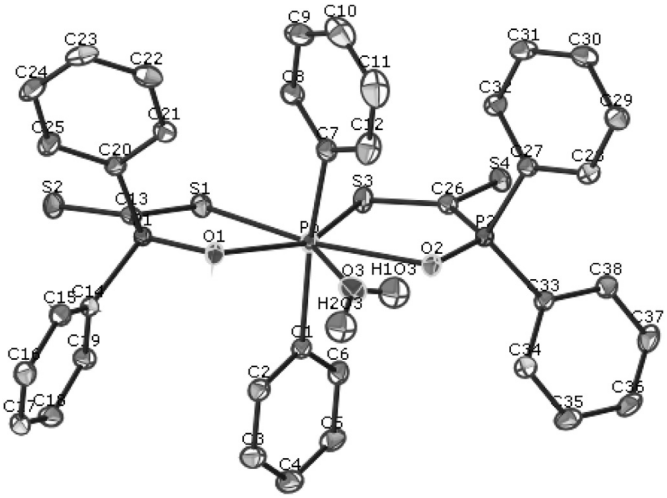

Fig. 1. Molecular structure of $[Ph_2Pb(L1)_2(H_2O)]$ 1.

Table 2
Selected bond distances and angles for **1**.

Bond distances, Å			
Pb bonds	S-C bonds	P-O bonds	P-C bonds
Pb-S1 2.769(1)	S1-C13 1.701(2)	P1-O1 1.506(1)	P1-C13 1.839(2)
Pb-S3 2.739(1)	S2-C13 1.651(2)	P2-O2 1.507(1)	P1-C14 1.800(2)
Pb-O1 2.435(5)	S3-C26 1.702(2)	O3-H 0.84	P1-C20 1.801(2)
Pb-O2 2.488(8)	S4-C26 1.649(2)	O1-H 1.83	P2-C26 1.845(2)
Pb-O3 2.628(6)			P2-C27 1.794(2)
Pb-C1 2.170(1)			P2-C33 1.799(2)
Pb-C7 2.170(3)			
Bond Angles, °			
O1-Pb-O2	134.1(8)	O1-Pb-O3	71.7(1)
S3-Pb-S1	74.8(1)	O3-Pb-O2	62.5(1)
O1-Pb-S1	75.7(3)	O3-H-O1	156.8
O2-Pb-S3	75.6(4)		
C1-Pb-C7	161.3(8)		

The two $[Ph_2P(O)CS_2]^-$ ligands in **1** coordinate in a bidentate manner in a trapezoidal way defining the equatorial plane with both S and both O atoms in *cis* positions. The O(1)-Pb-O(2) angle (134.1(8)°) is significantly larger than the S(1)-Pb-S(3) angle (74.8(1)°), and is bisected by the Pb-OH_2 bond. The range of angles within the equatorial plane is 62.5–75.7° adding up to 360.3° reflecting the essentially pbp coordination of Pb.

The Pb-S bond distances of 2.739(1) and 2.769(1) Å are comparable to bond distances found for sulfur ligands in the octahedral organometallic lead(IV) compounds, $[Ph_2Pb(S_2P(OBz)_2)_2]$ (2.679, 2.723 Å) [10] and $[Ph_2Pb(S_2PPh_2)_2]$ (2.656 Å).[4(d)] However, the Pb-S bond distances in **1** are somewhat longer than the Pb-S bond distances in the $[Ph_2Pb(L1)_2]$ octahedral compound that has Pb-S bond distances of 2.704(1) and 2.714(1) Å, presumably because of the larger coordination number of the lead atom in **1** [16].

The Pb-O(1) and Pb-O(2) bond lengths of 2.435(5) and 2.488(8) Å are comparable to the Pb-O bond distances found in $Ph_2Pb[(OPPh_2)_2N]_2$ and $Me_2Pb[(OPPh_2)_2N]_2$ (2.342(5) - 2.462(5) Å) [21], and compare well with distances observed in the octahedral structure of **1** [12]. The coordinated L2 shows considerable single bond character for the P-O bonds with bond distances of 1.506(1) and 1.507(1) Å indicating significant donation from oxygen atoms to the lead center. These distances are in between the single and double bond distances in $Ph_2P(O)OH$, where the P=O double bond distance is 1.486(6), and the P-O single bond distance is 1.526(6) Å) [22]. The bond distances of the P=O double bond in the free ligands, L1 and L2 are 1.492 and 1.488 Å [15], and quite similar to the P=O bond distance in Ph_3PO (1.483 Å) [23].

The Pb-OH_2 bond distance (2.628(6) Å) in **1** is significantly longer than the Pb-O1 and Pb-O2 distances as expected. The average Pb-O bond distances between the lead and oxygen atoms of the ligand is slightly longer than the sum of the covalent radii, but shorter than the sum of the van der Waals radii. The hydrogen atoms in the aqua ligand are hydrogen bonded to the oxygen atoms in the equatorial plane.

Blue crystals of $[MeHg\{S_2CP(O)Ph_2\}]$, **6′** suitable for X-ray diffraction were obtained by diffusion of diethyl ether into a petroleum ether solution of **6** at 4 °C. The distorted T-shape structure of **6′** is shown in Fig. 2. Fig. 2 depicts the ORTEP diagram of **6′** with displacement ellipsoids at 30% probability and the atom numbering scheme. The data refinement was not completed due to

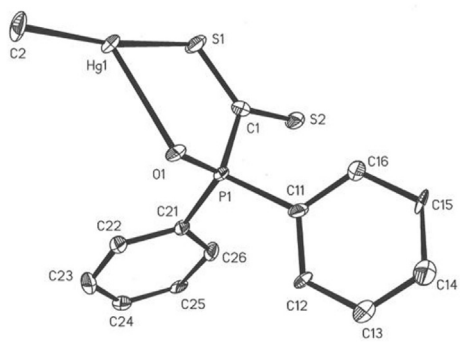

Fig. 2. Molecular structure of [MeHg(L1)] 6′.

deterioration of the crystal during data collection. Therefore, relevant data is provided in the supplementary section. Selected bond distances and angles for **6′** are listed in Table SI 2, and the crystallographic data collection information is given in the experimental section.

The mercury is observed in a near linear geometry with an apparent interaction with the oxygen atom of the P=O group. The ligand L1 is coordinated to the Hg(II) through one of the dithioformate sulfur atoms. The Hg(1)-S(1) bond distance of 2.405 Å compares well with those in the related compounds MeHg(S_2CNEt) [24] (2.418 Å), and MeHg(phen)·H_2O, (phen = phenicillamine) of 2.371 Å and 2.361 Å [25], and for MeHg(S_2PPh_2) [26] with Hg-S bond lengths of 2.379 Å. The C(2)-Hg(1) distance of 2.098 Å agrees well with those in the above referenced compounds with the C(2)-Hg(1) bond distances of 2.043, 2.076/2.095, and 2.081 Å respectively. These compounds represent known geometry for Hg(II) compounds where the Hg center exists in essentially linear coordination geometry but exhibits a secondary weak bond to sulfur in the solid state. The phosphinoyl oxygen of L2 is geometrically orientated in **6′** to form a five membered Hg-S-C-P-O ring. The observed distance between the mercury and the oxygen atom indicates presence of a secondary weak bond in the solid state with the Hg(1)-O(1) distance of 2.626 Å. This is longer than the covalent bond length but much shorter than the sum of the van der Waals radii of 3.23 Å between Hg and O atoms.

Comparable Hg-O bond lengths are found in MeHg(phen)·H_2O as 2.883 Å and 2.890 Å [25], and corresponding bond lengths found in phenylmercury(II) β-oxodithioesters, are 2.638(14) Å and 2.644(10) Å respectively [27]. This secondary Hg-O bond reduces the C-Hg-S angle to establish a distorted T-shaped structure around the Hg atom with the angles C(2)-Hg(1)-S(1), C(2)-Hg(1)-O(1) and S(1)-Hg(1)-O(1) equal to 169.7°, 107.9°, and 83.4°, respectively. The phosphorous-oxygen bond distance in **6′** is 1.511 Å, is slightly longer than is observed in **1,** confirming it has considerable single bond character. The C-S distances differ as expected with C(1)-S(1) distance of 1.711 Å for the sulfur bound to the mercury center, and 1.661 Å for the C(1)-S(2) bond, compared to the 1.675 Å found for the C-S double bond lengths in the free ligand [16]. This agrees well with the C-S bond distances in related compounds that show intermediate bond distances between single (1.82 Å), and double (1.56 Å) bonds [28]. In contrast to the compounds referenced above, the structure of **6′** does not show any evidence of intermolecular interactions. Typical intermolecular interactions through secondary Hg-S bonds are observed for phenylmercury(II) dithiocarbamate complexes with appended ferrocene ligands who form *aniso* bidentate dithiocarbamate structures with Hg-S bond distances of 3.23 Å and 3.08 Å reported for two different ligands [18]. Examination of the shortest intermolecular distance in **6′** showed the S(2)-Hg(2) distance as 3.80 Å or slightly longer than the sum of the van der Waals radii between Hg and S [29].

2.3. Infrared spectra

Table 3 shows the observed vibrational frequencies observed for $\tilde{\nu}$(P=O), $\tilde{\nu}$(C=S), $\tilde{\nu}$(C-S), $\tilde{\nu}$(P-S), and $\tilde{\nu}$(M − S). Infrared spectroscopy was used to determine the frequency shift with respect to the free ligands L1 and L2, to obtain information regarding the coordination geometry of the new compounds. In **1**, where the ligand is S,O-bidentate the P=O bond distance is 0.017 Å longer than observed in the free ligand [11], the $\Delta\tilde{\nu}$(P=O) shift is a useful diagnostic tool to study the bonding mode of $[R_2P(O)CS_2]^-$ ligands towards "R_3Pb(IV)" and "RHg(II)" metal fragments. The coordination shifts $\Delta\tilde{\nu}$(P=O) to lower frequency indicate formation of Pb-O bond as shown for (4) in Scheme 2, but coordination shifts of smaller magnitude point to secondary bonds with weaker donation of the oxygen atom to the Pb(IV) or Hg(II) center as shown in drawing (5) in Scheme 2. Coordination shifts to higher energy were confirmed in the synthesized dithioethers, $[Bz_2P(O)CS_2R]$ (R = Me, Et), where $\Delta\tilde{\nu}$(P=O) shift was observed in the range of +1 to +7 cm^{-1}.[1] The $\tilde{\nu}$(P=O) stretch is normally shifted by about 32–98 cm^{-1} towards lower energy when $[R_2P(O)CS_2]^-$ coordinates to the Ph_2Pb(IV) metal center [16]. The coordination shift, $\Delta\tilde{\nu}$(P=O) = $\tilde{\nu}$(compound) − $\tilde{\nu}$(ligand), is clearly dependent on the substituent on the phosphorous. Therefore, shifts of about $\Delta\tilde{\nu}$ = 39 - 46 cm^{-1} for L1, and 92–98 cm^{-1} observed for L2, are associated with Pb-O bond formation and S,O-bidentate coordination in the lead aryl compounds [16].

As shown in Table 3, $\Delta\tilde{\nu}$(P=O) for compounds with L1 (**2**, **3**, **6**) shift to lower energy suggesting *aniso*-bidentate coordination environment for the ligand $[Ph_2P(O)CS_2]^-$ as shown for (5), and (7) in Scheme 2 based on the magnitude of the shifts. The solid state structure for **6′** is S,O-bidentate as shown in Fig. 2. In agreement with reduced anisotropy of the dithioformate, $\tilde{\nu}$(C=S) is shifted by +8 cm^{-1} to higher wavenumber compared to $\tilde{\nu}$(C=S) in the free ligand. Comparable shifts to higher wavenumber are observed (Table 3) for **4**, **5**, and **7,** that therefore are expected to have similar bonding (Scheme 2(4)) as observed for **6'**.

Different behavior is observed for the aryl substituted compound **8**. Its coordination shift for $\tilde{\nu}$(P=O) is +1 cm^{-1} indicating L2 is monodentate or S,S-coordinated in the solid state. Compound **8** has different color, solubility, and a significantly higher melting point than **6** and **7**, emphasizing its difference in bonding and structure. Compound **8** likely has *aniso* bidentate S,S coordinated solid state structure similar to known [(aryl)Hg(S_2CNR_2)] compounds [30]. Asymmetrically substituted aryl mercury(II) dithiocarbamate compounds with methyl and benzyl ligands form *aniso*-bidentate S,S coordinated compounds that were reported to have comparable melting points. In these compounds, secondary Hg-S interactions and π interaction between Hg and the aryl ligands result in strong intermolecular interactions and, presumably, in higher melting points [30]. Compounds **2** and **4**, with methyl ligands, show limited solubility in non-coordinating solvents whereas all the other compounds are reasonably soluble in $CHCl_3$ or CH_2Cl_2. The lack of solubility suggests **2** and **4** have polymeric structures as shown for (7) in Scheme 2 with intermolecularly bonded ligands. IR spectra confirm the bonding must the bidentate S,O bonding. Known aryl, and methyl substituted lead compounds, $[Ph_3Pb(S_2PMe_2)]_n$ [11] and $[Me_3Pb(O_2PPh_2)]_4$ [10] were found to exhibit chain polymeric and tetrameric molecular structures and similarly show limited solubility in noncoordinating solvents. In the [PhHg(S_2CN(Me)(N-methylpyridine)] complex, the mercury center atom forms *aniso*-bidentate S coordination with the dithiocarbamate and additional intermolecular Hg-N secondary bonding resulting in chain polymeric structures [30].

Table 3
Selected IR data for the ligands and their compounds.[a]Shown in cm^{-1}.

Compound	$\tilde{\nu}$(P=O)	$\Delta\tilde{\nu}$(P=O)	$\tilde{\nu}_1(CS_2)$	$\tilde{\nu}_2(CS_2)$	$\tilde{\nu}$(Pb-S)/$\tilde{\nu}$(Hg-S)	$\tilde{\nu}$(Hg-Me)/$\tilde{\nu}$(Hg-Ph)
L1[b]	1176(vs)		1032(vs)	915(w)		
L1[c,d]	1168(vs)		1034(vs)			
L2[b]	1200(vs)		1030(vs)	910(w)		
1	1138(vs)	−38	1040(vs)	903(s)	378(s)	
1[c]	1139(vs)		1042(vs)	904(w)		
2	1157(vs)	−19	1056(vs)	890(w)	360(m)	
3	1160(vs)	−16	1048(vs)	898(m)	386(s)	
4	1165(vs)	−35	1040(vs)	912(m)	360(m)	
5	1160(vs)	−40	1048(vs)	912(s)	366(m)	
6	1155(s)	−21	1047(s)	900(m)	315(m)	540(m)
6[c]	1185/1155(m)		1055(vs)	904(w)		
7	1170(s)	−30	1040(s)	910(m)	312(m)	542(s)
7[(c)]	1185/1167(m)		1049(vs)	912(w)		
8	1201(vs)	1	1056(vs)	918(s)	220(m)	455(m)

[a] Spectra recorded in KBr pellets.
[b] (PPh_4)[L], ref [16].
[c] In $CHCl_3$.
[d] (Et_4N)[L1], ref [40].

2.3.1. Solution IR spectra of selected compounds

IR was obtained of L1, and of compounds, **1**, **6** and **7** as chloroform solutions. The bands associated with L1 shift in general no more than ±4 cm^{-1} or within the error of the measurement. This is in agreement with reported data for other dithioformate ligands in KBr and in chloroform solution.[4c)] Absorptions arising from the P=O group and the CS_2 group in the complexes are expected to behave accordingly unless a change in the coordination mode of the ligand takes place in solution. Chloroform has a strong absorption at 1200 cm^{-1} obscuring any overlapping absorbances.

Table 3 lists the absorbances observed from the P=O and CS_2 groups in KBr and in $CHCl_3$ for selected compounds. The IR spectra of **L1** and of **1** are not significantly different in the solid state and in solution. The second weak absorption from the CS_2 group was not observed in $CHCl_3$ for **L1** presumably due to free rotation and absence of electrostatic interactions in solution. The results are in agreement with our NMR data showing the oxygen is coordinated to the lead center in solution for **1**.

Compounds **6** and **7** show two absorbances for the phosphinoyl group in solution. One absorbance is shifted to higher energy indicating weaker Pb-O coordination while the other one is indistinguishable from the solid state peak position. For **6** the higher energy band at 1185 cm^{-1} is higher than in **L1** confirming this species does not have S,O coordinated ligand and that two species are present in solution. The higher energy CS_2 group absorbance is shifted to higher energy by 8 and 9 cm^{-1} respectively. The second CS_2 absorbance at around 900 cm^{-1} is weak and shows shifts that do not significantly differ from the KBr absorbances and are therefore most likely from the S,O bonded species. It may be deduced that the second species in solution is S,S bonded and largely isotropic. The spectra support that two species are present in solution as would be expected for non-rigid behavior and both S,O and S,S coordinated compounds are present.

2.3.2. The far-IR spectra

The far-IR spectra of the compounds **1**–**8** show medium intensity vibrations in the region of 312–386 cm^{-1}. These vibrations were assigned to the Pb-S and Hg-S bond stretching modes since they are absent in the spectra of the free ligands and starting materials. Frequencies at 540 cm^{-1}, 542 cm^{-1}, and at 455 cm^{-1} for **6**, **7**, and **8**, respectively were assigned to the Hg-C stretching modes. Comparable values of $\tilde{\nu}$(Hg-C) were reported at 522 cm^{-1} for the compound $[MeHg(S_2CNEt_2)]$ [24], and at 529 cm^{-1} for the $[MeHg(S_2PPh_2)]$ compound [26].

2.4. Electronic spectra

Data is provided in the experimental section. The free ligands exhibit an intense absorption (log$\varepsilon \approx 4$) at 365 nm that is assigned as a π to π^* transition of the dithioformate group. The phosphinoyldithioformates show two absorption maxima of low intensities at 480 nm and at 555 nm, which are responsible for the color of the compounds and were assigned to n - π^* transitions of the P(=O)-CS_2 group. Normally, dithiocarboxylates XCS_2^- (X = NR_2, OR, SR) show one n - π^* transition in their electronic spectrum [29]. Appearance of two n - π^* absorbances indicates delocalization of π-electrons in the P-C bond and mixing of d-electrons of the phosphorous with the π-system of the CS_2-moiety. Presumably, the transitions at 480 nm possess larger contribution from the n - π^* absorption in the CS_2 system whereas the absorption at 555 nm has energy closer to the P=O chromophore. The colors of the alkyl mercury compounds are violet, and blue respectively, whereas the aryl mercury compound is pink. The lead compounds **2**–**5** are orange-red, and **1** is purple.

2.5. NMR spectroscopy

NMR spectra of the ^1H, ^{13}C, and ^{31}P nuclei were analyzed to verify the coordination mode of the metal atom based on coupling constants and chemical shifts.

2.5.1. ^1H and ^{13}C NMR data

The NMR spectra of compounds **1**–**8** exhibit resonances from the organic groups bonded to the lead, mercury, and phosphorous atoms confirming the identity of the compounds. The ^1H and ^{13}C NMR data are presented in Tables 4 and 5 and in the experimental section. Scheme 7 shows numbering scheme for ^{13}C NMR spectra. All compounds were analyzed in $CDCl_3$ or CD_2Cl_2, except for **2** and **4** who were analyzed in dmso-d_6 because of their limited solubility.

The ^1H NMR spectra of the benzyl groups in the "$(Bz)_2P$" moiety exhibit one set of signals for the protons as well as for the carbon atoms in compounds **4**, **5**, **7**, and **8** indicating the presence of a mirror plane in the molecules rendering them chemically equivalent. Presence of coupling of phosphorous nucleus and the aromatic protons observed in L1 gives rise to ^2J, ^3J, and ^4J coupling constants as well as ^5J coupling to the *para* protons. Coupling constants between the phosphorous nucleus and the aromatic protons in L2 were not determined because the signals were obscured.

Table 4
Selected ^{1}H NMR data in CD_2Cl_2 or as stated.[a]

Compd.	P-$CH_\alpha H_\beta$	P- C_6H_5 or P-C_0-C_6H_5, (H_o, H_m, H_p)	M – C_6H_5 or M-R (M = ^{207}Pb or^{199}Hg; R = Me, Et);
1		7.42 (m), 7.26 (m) H_p(obsc.) 7.8 ^3J(P-H_o), 3.6 ^4J(P-H_m)	8.05 (m), 7.40 (m), H_p(obsc.), 187 ^3J(Pb-H_o), 73 ^4J(Pb-H_m)
2[a]		7.8 (m), 7.4–7.6 (m)	0.716 (ss, 9H), 81.1 ^2J(Pb-H)
3		7.81 (m), 7.41 (m), 7.53 (m), 11.6 ^3J(P-H_o), 3.2 ^4J(P-H_m), 1.5 ^5J(P-H_p)	2.17 (qs), 1.73 (ts, 9H), 39.8 ^2J(Pb-H_α), 175 ^3J(Pb-H_β)
4	3.58(dd, H_a), 3.41(dd, H_b), 12.6 ^2J(P-H_a), 13.7 ^2J(P-H_b), 14.2 ^2J(H_aH_b)	7.3–7.2 (m)	1.72 (ss, 9H), 65.3 ^2J(Pb-H)
5	3.66(dd, H_a), 3.43(dd, H_b), 12.7 ^2J(P-Ha), 13.4 ^2J(P-Hb), 14.1, ^2J(HaHb)	7.3–7.2 (m)	2.10 (qs, 6H), 1.72 (ts, 9H), 38.2 ^2J(Pb-H_α), 175 ^3J(Pb-H_β)
6		7.84 (m), 7.59 (m), 7.47 (m), 11.8 ^3J(P-H_o)	1.04 (ss, 3H), 189.7 ^2J(Hg-H)
7	3.53 (dd, H_a), 3.45 (dd, H_b), 12.0 ^2J(P-H_a), 14.0 ^2J(P-H_b), 14.0, ^2J(H_aH_b)	7.3–7.2 (m)	0.792 (ss, 3H), 191.6 ^2J(Hg-H)
8	3.56 (dd, H_a), 3.45 (dd, H_b), 12.0 ^2J(P-H_a), 14.0 ^2J(P-H_b), 14.1, ^2J(H_aH_b)	7.3–7.2 (m, 10H)	7.37 (m, 2H), 7.40 (m, 2H), H_p(*obsc.*) 177.6 ^2J(Hg-H_o), 72.0 ^4J(Hg-H_m)

[a] In dmso-d_6. (b) ss: singlet surrounded by singlet satellites. ts: triplet surrounded by triplet satellites. qs: quartet surrounded by quartet satellites. *obsc*: obscured.

Table 5
$^{13}C\{^1H\}$ NMR data [δ, ppm, J(Hz)] for the compounds and the free ligands.[a]

Cmpd	C_O, [^1J(^{31}P,C_O)]	C_7, [^1J(^{31}P,C_7)]	Cα or C8, [1J(M,Cα)] or [1J(M,C8)][a]	Cβ, or $C_{9,10,11}$, [^nJ(^{31}P,Cβ)] or [^nJ(^{31}P,$C_{9,10,11}$], $^{(\alpha)}$
L1[b]		253.8 [71.6]		
L2[b]	36.3 [60.5]	257.7 [62.1]		
1		249.2 [69.8]	168.3 [1210]	134.3, 130.6, 130.2 [120.7, 180.0, 38.0]
2[c]		249.8 [69]	19.1 [340]	
3		249.2 [69.8]	31.6 [216.4]	13.6 [41.8]
4[c]	35.2 [64]	250.0 [54.0]	19 [338]	
5	37 [62.6]	249.9 [58.2]	31.8 [212.9]	14.1 [43.0]
6		249.6 [66.0]	7.93 [1411]	
7	36.7 [64.0]	250.3 [54.8]	7.1 [1441]	
8	36.7 [64.3]	249.9 [54.3]	155.8 [2233]	136.8, 128.7, 128.5 [110.6, *obsc.*]

[a] M = ^{207}Pb or^{199}Hg.
[b] From ref. [16].
[c] In dmso-d_6.

Both ^{207}Pb and ^{199}Hg nuclei couple with the alkyl or aryl ligand protons. The 7-coordinate compound **1** shows exactly the same chemical shifts and coupling constants as the 6-coordinate [$Ph_2Pb(L1)_2$] [16], indicating the loss of H_2O ligand in dilute $CDCl_3$ solutions. The methylene protons in the benzyl groups of **4**, **5**, **6,** and **7** are chemically non-equivalent. The signal for H_α is observed in the range of δ = 3.13–3.56 ppm and for H_β between δ = 3.41–3.45 ppm. Both protons exhibit geminal coupling with phosphorous giving rise to eight lines in the ^{1}H spectrum for the H_aH_b signal.

The ^{13}C NMR data show a general behavior where coupling is observed between the lead and the *ipso* or *alpha* carbon on the organometallic ligand and between the phosphorous and the C_7 carbon, and between the phosphorous and the carbon atoms on the phenyl or benzyl groups respectively. Presence of ^{31}P-^{13}C couplings allowed determination of coupling constants for ^2J, ^3J and ^4J for both ligands as well as for ^5J in L2.

In general, the coordination geometry of the *di*- and *tri*-aryl lead(IV) complexes is reflected in the NMR parameters [10,16,31]. Thus, the magnitude of the coupling constants in the hexa-, penta-, and tetracoordinate lead(IV) complexes, [$Ph_2Pb(L2)_2$], [$Ph_2PbCl(L2)$], and [$Ph_3Pb(L2)$][16] exhibit the values 1188, 908 and 562 Hz, for ^1J(^{207}Pb,^{13}C), respectively in their ^{13}C NMR spectra, and 187, 168 and 106 Hz, for ^3J(^{207}Pb,^{1}H), respectively in their ^{1}H NMR spectra. Values of 341.4 Hz (^1J(^{207}Pb,^{13}C)) and 79.3 Hz (^2J(^{207}Pb,^{1}H)), were reported for [$PbMe_3\{(OPPh_2)_2N\}$] and 391.7 Hz (^1J(^{207}Pb,^{13}C)) and 85.7 Hz (^2J(^{207}Pb,^{1}H)) for [$PbMe_3(O_2PPh_2)$] confirming the existence of the "Me_3Pb" moiety in the compounds [10]. Values for ^1J(^{207}Pb,^{13}C) and ^3J(^{207}Pb,^{1}H) coupling constants are generally smaller for organometallic alkyl substituents than for the aryl substituted compounds [32]. Compounds **2**, **3**, **4**, and **5**, show coupling constants in the range of 212.9 Hz–340 Hz for J(^{207}Pb,^{13}C) in agreement with a reported 4 coordinate geometry. They are, therefore, considered adopting 4-coordinate monomeric structures

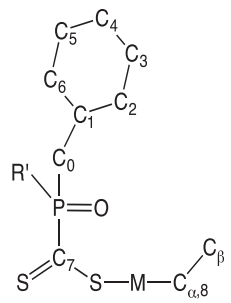

Scheme 7. Carbon atom numbering.

in solution and L1 and L2 are acting as monodentate S-donors (Scheme 2 (1)).

The coupling constants for the coupling of the metal nucleus with the *ortho* and *meta* protons of the phenyl ligand in **1** and **8** (Table 4) were determined. The coupling constants for $^2J(M,^1H_o)$ in **1**, and **8** are 191 Hz and 187 Hz, respectively, and the corresponding $^3J(M,^1H_m)$ coupling constants are 73 Hz and 45 Hz. The phenyl groups in **1** are *trans* to each other (linear). Comparable coupling constants are expected for similar geometric arrangements of the organometallic ligand, and based on that **8** assumes coordination number of two in solution at ambient temperature.

The ^{1}H and ^{13}C NMR spectra for compounds **6**, **7** and **8** are in agreement with the composition deduced from the synthesis and the elemental analysis (Tables 5 and 6). The most significant coupling constants, $^2J(^{199}Hg, ^1H)$ and $^1J(^{199}Hg,^{13}C)$ were found to be 189.7 Hz and 1411 Hz for **6**, and at 191.6 Hz and 1411 Hz for **7**. The corresponding coupling constants in [HgMe(S_2COEt)] were found to be 183.3 Hz and 1339.0 Hz where the ethyl xanthate is coordinated in an *aniso*-bidentate manner in the solid state [31]. In **8**, the coupling constants $^3J(^{199}Hg,^1H)$ and $^1J(^{199}Hg,^{13}C)$, for the Hg(II) to H_o proton coupling and for the Hg(II) to the phenyl *ipso* carbon coupling constants were determined as 177.6 Hz and 2233 Hz respectively. The coordination of L1 and L2 is confirmed by considerable upfield shift of both the CS_2 signal and the signal for C_i. The CS_2 carbon is observed as a doublet at very low field, and $\delta(CS_2)$ is at about 250–260 ppm. The $^1J(^{31}P, ^{13}C_7)$ coupling constant for all of the compounds is on the order of 55–70 Hz.

2.5.2. ^{31}P NMR data

The ^{31}P NMR spectra show a single resonance for the phosphorous nucleus in solution at ambient temperature (298 K) for all of the compounds. The chemical shifts for the ^{31}P NMR spectra are presented in Table 1. The phosphorous in L1 appears at a lower chemical shift than in L2 with respect to the reference. The alkyl groups do not significantly affect the ^{31}P NMR chemical shifts. Coupling between the metal and phosphorous is observed only for compound **1** confirming coordination of the oxygen to the lead in solution. The coupling constant of 90 Hz is in good agreement with the six-coordinate version of **1** suggesting the coordinated water molecule is a solid state phenomena. The absence of the ^{207}Pb to ^{31}P coupling along with the magnitude of the $^1J(^{207}Pb,C\alpha)$ coupling constants obtained in the ^{13}C NMR spectra confirms the preferred coordination for the alkyl compounds **2**–**5**, as monodentate sulfur coordination in solution.

Table 6
Variable temperature^{31}P NMR data for **6**, [HgMe(L1)], in CD_2Cl_2.

Temperature K	Low field signal/ppm (Δν½/Hz),[a] [integral/%]	High field signal/ppm (Δν½/Hz),a) [integral/%]
283		27.2(17)
265		27.2(56)
245		26.2(120)
230	31.8 [19]	25.9(29) [81]
215	31.8(77) [22]	25.9(25) [78]
200	31.6(28)	25.9(18)
190	31.5(24) [25]	25.9(18) [75]

[a] Full width at half maximum (fwhm).

2.5.3. Variable temperature ^{31}P NMR study

The Hg(II) compounds are highly soluble in non-coordinating solvents and behave as discrete molecules. The crystal structure of **6′** shows the Hg atom is involved in an intramolecular interaction with the phosphinoyl oxygen and the shift of the phosphinoyl stretch in the infrared spectrum confirms this to be a bulk property. It was unexpected to see preference for secondary O interaction rather than *aniso* sulfur bidentate coordination. As a soft Lewis acid the [MeHg(II)]+ species is expected to prefer sulfur donors. The ambidentate nature of the ligands in parallel with known tendency of Hg(II) compounds to form T-shaped molecules with *aniso* S,S bidentate coordination in dithiocarbamates [18,19,30] invoked the question of a possible non-rigid behavior in solution, and possible detection of the expected *aniso* S,S coordinated species at low temperature. To explore this in more detail, the ^{31}P NMR of **6** was studied as a function of temperature. As shown in Table 1, none of the compounds **6**–**8** show coupling between the ^{199}Hg and ^{31}P indicating that the oxygen donor is dissociated in solution although the $^1J(^{199}Hg,C\alpha)$ coupling constants obtained in the ^{13}C NMR spectra are larger than expected for a linear geometry. The Pb(IV) compounds, **6** and **7,** exhibit very similar coupling constants $^1J(^{199}Hg,^{13}C\alpha)$ and of comparable magnitude to [MeHg(S_2COEt)] which is T-shaped with an *aniso* S,S bidentate dithiocarbamate ligand [33]. We concluded that **6**, and **7** likely exhibit non-rigid behavior in solutions where a rapid equilibrium between the S,O and the *aniso* S,S coordination obscures possible detection of coupling between the ^{199}Hg and ^{31}P as judged from considerable line broadening of the $^{31}P\{^1H\}$ NMR signal upon cooling. Variable temperature study of the ^{31}P spectrum was performed for **6′** in CD_2Cl_2. Results from this ^{31}P NMR study are shown in Table 6 and in Fig. 3. Scheme 8 shows suggested conformational equilibrium of an *aniso* bidentate S,S coordination and bidentate S,O-coordination.

A solution of **6** shows a single resonance at 27.2 ppm and 283 K. The signal broadens upon cooling until 230 K. Non-rigid behavior is revealed where a second resonance appears downfield and the major resonance shifts upfield to 25.9 ppm and becomes sharp. The new resonance is at 31.5 ppm. Cooling further shows a small increase in the new resonance to occur, and a significant narrowing of the resonance at half height. The signal at 25.9 ppm is the major resonance, and further cooling to 190 K only brings the ratio to just below ¼ vs. ¾ indicating that the S,S coordination is minor in solution and that the S,O coordination is favored. The molecular structure of **6′** is T-shape with the Hg-O bond distance of 2.626 Å suggesting that the $[MeHg(II)]^+$ species prefers the S,O coordination. This unexpected preference for S,O coordination may be explained by considering that the methyl group is a small ligand and that the five membered ring has both larger bite angle and less ring strain than the four membered *aniso* S,S coordinated ligand provides.

Dynamic NMR simulations of the P signals using the software WinDNMR [34] as shown in Fig. 3 allowed determination of the rate constants $\boldsymbol{k_{6\text{-}6'}}$ and the corresponding free energies of activation

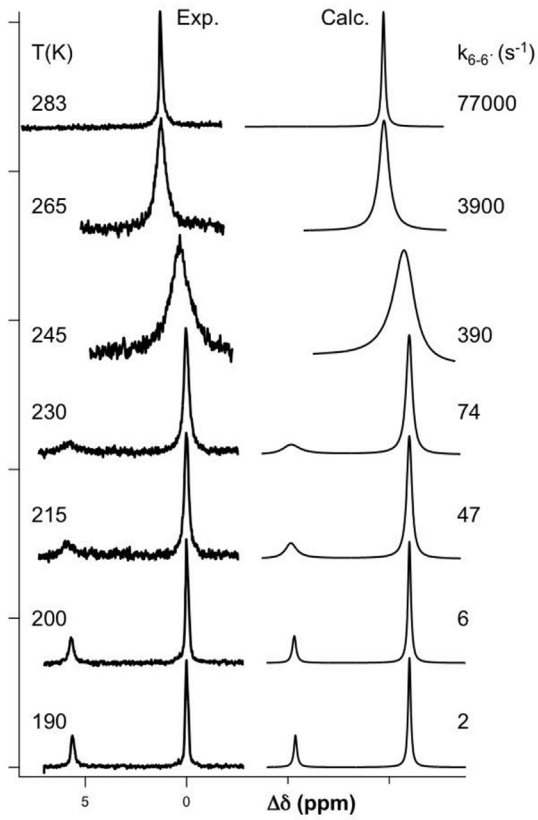

Fig. 3. Variable temperature ^{31}P NMR spectra of 6-6'. Simulated spectra are shifted to the right side of the experimental spectra for clarity reason.

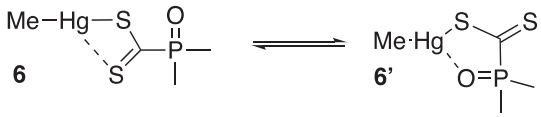

Scheme 8. Conformational equilibrium of 6 and 6'.

($\Delta G^{\#}_{\mathbf{6\text{-}6'}}$) as a function of temperature. Chemical shifts, derived from the ^{31}P NMR spectra, which were recorded at the lowest temperature were assumed to represent conditions of negligible interconversion. An average value for $\Delta G^{\#}_{\mathbf{6\text{-}6'}} = 45.7 \pm 1.7$ kJ mol^{-1} was obtained for the temperature range of 190 K–283 K. Furthermore, the equilibrium constant ($\mathbf{K_{6\text{-}6'}}$) and the free energy difference ($\Delta G_{\mathbf{6\text{-}6'}}$), for the **6** to **6′** transformations, corresponding to 238 K (a temperature close to the coalescence point) were determined from the relative integrated signal intensities ($\mathbf{K_{6\text{-}6'}} = 0.28$ and $\Delta G_{\mathbf{6\text{-}6'}} = 2.5$ kJ mol^{-1}).

3. Conclusions

The ligands employed are well suited to study coordination preferences of Lewis acids. Organometallic alkyl compounds of lead(IV) and mercury(II) show interesting structural diversity in the solid versus the solution state when combined with L1 and L2. A clear difference in their solid state and solution coordination mode preferences is observed. Several organometallic alkyl Pb(IV) compounds show S,O bidentate coordination preference in the solid state whereas monodentate sulfur coordination is preferred in solution. In solution the Pb(IV) compounds with methyl ligands form S,S coordinated intramolecular polymeric structures. The other Pb(IV) compounds favor monodentate S-coordination. Comparable compounds with aryl ligands maintain their S,O bidentate coordination in solution [16].

The aryl Hg(II) compound **8** prefers *aniso* S,S coordination in solid and solution state as expected for a soft Lewis acid and the softer sulfur donor. The bulkier organometallic aryl ligand leads to formation of an *aniso* S,S coordination that may be attributed to the smaller bite angle of the S,S bidentate coordination. Compounds reported here with alkyl Hg(II) fragments show an unexpected S,O bidentate coordination preference in the solid state exhibiting non-rigid behavior in solution.

These studies confirm that although oxygen is favored over sulfur as a second electron donor from the phosphinoyldithioformate ligand in the solid state, non-rigid behavior transforming to *aniso* S,S bidentate coordination occurs. This is confirmed by low temperature DNMR studies for **6** and solution IR spectra of **6** and **7**. The non-rigid behavior showcases the versatility of the $[S_2CP(O)R_2]^-$ ambidentate ligand where the oxygen donor may dissociate and coordinate depending upon external conditions.

4. Experimental section

General Considerations. Me_3PbCl, Et_3PbCl, MeHgCl and PhHgCl were purchased from Ventron Corporation and used as such after vacuum drying or distillation. K[L1]·dioxane, (PPh_4)[L1]·$0.5H_2O$, K[L2] and (PPh_4)[L2] were prepared by published methods [35]. Solvents were purified using standard procedures. Anhydrous solvents were purchased from Aldrich and used as received.

Infrared spectra were obtained with a Perkin-Elmer 283 spectrophotometer in the range of 4000–200 cm^{-1} using KBr/CsI pellets. UV–visible spectra were recorded on Ultraspec3000 or Perkin-Elmer Lambda 17 spectrometers. Elemental analyses were carried out on a Carlo Erba Strumentazione model 1106 analyzer. All NMR spectra were recorded on a Bruker AC-250 spectrometer operating at 250.133, 101.256 and 62.896 MHz for ^{1}H, ^{31}P-{^{1}H}, and ^{13}C-{^{1}H} respectively and at 298 K unless otherwise noted. The deuterated solvent served as the lock in the ^{1}H and ^{13}C measurements with chemical shifts referenced to tetramethylsilane or tetramethylplumbane. The ^{31}P NMR spectra were calibrated against an external 85% H_3PO_4 aqueous solution. High frequency positive convention was used for all chemical shifts.

Procedures. [$Ph_2Pb\{S_2CP(O)Ph_2\}_2$] (1). Synthesis was as published previously [16]. Single crystals were grown by diffusion of ether into a dichloromethane solution. The solvents were not dried to remove water. Purple crystals were collected and air dried.

[$Me_3Pb\{S_2CP(O)Ph_2\}$] (2). Methanol was added in 5 ml portions to a stirred solution of (PPh_4)[L1]·$0.5H_2O$ (0.385 g, 0.615 mmol) and $PbMe_3Cl$ (0.158 g, 0.615 mmol) in CH_2Cl_2 (15 ml). The orange-red solution gradually turned red-brown and a red precipitate started to form after addition of about 40 ml. The CH_2Cl_2 was removed under reduced pressure and the mixture kept at 5 °C for 2 h. The resulting red powder was collected by filtration in air, washed with methanol and dried *in vacuo*. Yield: 0.250 g, 77%. Calc. for $C_{16}H_{19}OPS_2Pb$: C, 36.28; H, 3.62. Found: C, 36.22; H, 3.66. M.p.: 107–108 °C (dec.). IR (KBr, cm^{-1}): 1157 (vs) [$\tilde{\nu}$(P=O)], 1056 (vs) and 890 (w) [$\tilde{\nu}$(CS_2)]. ^{1}H NMR (CD_2Cl_2, *J*/Hz): δ 7.8 (4H, m, H_o of C_6H_5), 7.4–7.6(6H, m, H_m and H_p of C_6H_5), 0.716 (9 H, ss, $^2J_{Pb,H}$ 62.2, CH_3). ^{13}C NMR (dmso-d_6, *J*/Hz): δ 19.1[*J*(C- [31]P) 340], 130.2, 131.9, 128.7, 132.7[*J*(C_n-^{31}P) 105.6, 9.1, 12.2, 2.7], 230 [*J*(C_7-^{31}P) 70.0].

[$Et_3Pb\{S_2CP(O)(Ph)_2\}$] (3). A solution of K[L1]·dioxane (0.450 g, 1.11 mmol) in acetone (40 ml) and $PbEt_3Cl$ (0.337 g, 1.11 mmol) in acetone (20 ml). The solution changed from colorless to red and a white precipitate (KCl) was formed, which was filtered off after 30 min. 2-propanol (15 ml) was added and the acetone removed

under reduced pressure. The mixture was refrigerated overnight and the resulting orange-red powder collected by filtration in air, washed with 2-propanol and dried *in vacuo*. Yield: 0.514 g, 81%, red-orange powder. Calc. for $C_{19}H_{25}OPS_2Pb$: C, 39.92; H, 4.41. Found: C, 39.22; H, 4.32. IR (KBr, cm^{-1}): 1160 (vs) [$\tilde{\nu}$(P=O)], 1048 (s) and 898 (m) [$\tilde{\nu}$(CS_2)]. UV–vis (CH_2Cl_2, λ/nm, ε/$M^{-1}\cdot cm^{-1}$): λ 529 (n→π*, logε 1.61), 357 (π→π*, logε 3.79). ^{1}H NMR (CD_2Cl_2, *J*/Hz): δ 7.81 (4 H, m, $^3J_{P,H}$ 11.6, H_o of C_6H_5), 7.53 (2 H, m, $^5J_{P,H}$ 1.5, H_p of C_6H_5), 7.41 (4 H, m, $^4J_{P,H}$ 3.2, H_m of C_6H_5), 2.17 (6 H, q, sat, $^2J_{Pb,H}$ 39.8, CH_2CH_3), 1.73 (9 H, t, sat, $^3J_{Pb,H}$ 175, CH_2CH_3). ^{13}C NMR (CD_2Cl_2, *J*/Hz): δ 31.6[*J*(Cα-^{31}P) 216.4], 13.6[*J*(Cβ-^{31}P) 41.8], 132.4, 132.5, 128.4, 132.2[*J*(C_n-^{31}P) 103.1, 9.2, 12.0, 2.8], 249.2 [*J*(C_7-^{31}P) 69.8].

[$Me_3Pb\{S_2CP(O)(CH_2Ph)_2\}$] (4). Similar procedure as for **1** using $PPh_4S_2CP(O)(CH_2Ph)_2$ (0.370 g, 0.574 mmol) and $PbMe_3Cl$ (0.148 g, 0.575 mmol). Yield: 0.270 g, 84%, red-orange microcrystals. Calc. for $C_{18}H_{23}OPS_2Pb$: C, 38.77; H, 4.16. Found: C, 38.80; H, 4.19. M.p.: 130–131 °C (dec.). IR (KBr, cm^{-1}): 1165 (vs) [$\tilde{\nu}$(P=O)], 1040 (vs) and 906 (m) [$\tilde{\nu}$(CS_2)]. ^{1}H NMR (CD_2Cl_2, *J*/Hz): δ 7.3–7.2 (10 H, m, C_6H_5), 3.58 (2H, dd, $^2J_{P,H}$ 12.6, $^2J_{H,H}$ 14.2, H_a of CH_2Ph), 3.41 (2H, dd, $^2J_{P,H}$ 13.7, $^2J_{H,H}$ 14.2, H_b of CH_2Ph), 1.72 (9H, s, sat, $^2J_{Pb,H}$ 65.3, CH_3). ^{13}C NMR (CD_2Cl_2, *J*/Hz): δ 19.0 [*J*(Cα,^{31}P) 338.0], 35.2[*J*(C_0-^{31}P) 64.0], 130.6, 129.4, 127.7, 126.2 [*J*(C_n-^{31}P) 8.5, 5.6, 2.5, 2.9], 239.5 [*J*(C_7-^{31}P) 62.3].

[$Et_3Pb\{S_2CP(O)(CH_2Ph_2\}$] (5) Similar procedure as for **2** reacting $KS_2CP(O)(CH_2Ph)_2$ (0.430 g, 1.25 mmol) in acetone (40 ml) and $PbEt_3Cl$ (0.412 g, 1.25 mmol) in acetone (20 ml). Yield: 0.560 g, 75%, orange microcrystals. Calc. for $C_{21}H_{29}OPS_2Pb$: C, 42.05; H, 4.87. Found: C, 41.40; H, 4.81. M,p.: 129.5–130.5 °C (dec.). IR (KBr, cm^{-1}): 1160 (vs) [$\tilde{\nu}$(P=O)], 1048 (vs) and 912 (s) [$\tilde{\nu}$(CS_2)]. UV–vis (CH_2Cl_2, λ/nm, ε/$M^{-1}\cdot cm^{-1}$): λ 526 (n→π*, logε 1.54), 353 (π→π*, logε 3.87). ^{1}H NMR (CD_2Cl_2, *J*/Hz): δ 7.3–7.2 (10 H, m, C_6H_5), 3.66 (2 H, dd, $^2J_{P,H}$ 12.7, $^2J_{H,H}$ 14.1, H_a of CH_2Ph), 3.43 (2 H, dd, $^2J_{P,H}$ 13.4, $^2J_{H,H}$ 14.1, H_b of CH_2Ph), 2.10 (6 H, q, sat, $^2J_{Pb,H}$ 38.2, CH_2CH_3), 1.72 (9 H, t, sat, $^3J_{Pb,H}$ 175, CH2*CH*3. ^{13}C NMR (CD_2Cl_2, *J*/Hz): δ 31.8[*J*(Cα,^{31}P) 212.9], 14.1 [*J*(Cβ-^{31}P) 43.0], 37.0[*J*(C_0-^{31}P) 62.6], 132.2, 130.6, 128.8, 127.2 [*J*(C_n-^{31}P) 8.0, 5.2, 2.4, 3.0], 249.9 [*J*(C_7-^{31}P) 58.2].

[$MeHg\{S_2CP(O)Ph_2\}$] (6). K[L1]·dioxane (1.13 g, 2.79 mmol) and HgMeCl (0.76 g, 3.03 mmol) were filled in a Schlenk flask under N_2, 30 ml ether added and the suspension stirred for 10 min. The solution gradually turned blue and a white precipitate (KCl) started to form. The mixture was filtered giving clear blue solution. The solution was carefully concentrated under reduced pressure and placed in a refrigerator overnight. The resulting blue crystalline product was collected by filtration, washed with a mixture of ether and petroleum ether and dried in *vacuo*. Yield: 0.81 g, 59%, blue crystals. Calc. for $C_{14}H_{13}OPS_2Hg$: C, 34.1; H, 2.66. Found: C, 34.2; H, 2.63. M.p.: 98–99 °C (dec.). IR (KBr, cm^{-1}): 1155 (s) [$\tilde{\nu}$(P=O)], 1047 (s) and 900 (m) [$\tilde{\nu}$(CS_2)]. UV–vis (CH_2Cl_2, λ/nm, ε/$M^{-1}\cdot cm^{-1}$): λ 559 (n → π*, logε 1.46), 358 (π → π*, logε 4.00). ^{1}H NMR (CD_2Cl_2, *J*/Hz): δ 7.84 (4 H, m, $^3J_{P,H}$ 11.8, H_o of C_6H_5), 7.59 (2 H, m, H_p of C_6H_5), 7.47 (4 H, m, H_m of C_6H_5), 1.04 (3 H, s,sat, $^2J_{Hg,H}$ 189.7, CH_3). ^{13}C NMR (CD_2Cl_2, *J*/Hz): δ 7.93[*J*(Cα-^{31}P) 1411], 130.8, 132.7, 128.8, 132.8 [*J*(C_n-^{31}P) 106.9, 9.5, 12.4, 2.4], 249.6 [*J*(C_7-^{31}P) 66.0].

[$MeHg\{S_2CP(O)(CH_2Ph)_2\}$] (**7**) Same procedure as for **6** using K[L2] (1.17 g, 3.40 mmol) and HgMeCl (0.85 g, 3.39 mmol) in ether (40 ml). Yield: 1.10 g, 62%, violet crystals. Calc. for $C_{16}H_{17}OPS_2Hg$: C, 36.9; H, 3.29. Found: C, 36.9; H, 3.23. M.p.: 106–107 °C (dec.). IR (KBr, cm^{-1}): 1170 (s) [$\tilde{\nu}$(P=O)], 1040 (vs) and 910 (m) [$\tilde{\nu}$(CS_2)]. UV–vis (CH_2Cl_2, λ/nm, ε/$M^{-1}\cdot cm^{-1}$): λ 553 (n → π*, logε 1.51), 357 (π → π*, logε 4.02). ^{1}H NMR (CD_2Cl_2, *J*/Hz): δ 7.3–7.2 (10 H, m, C_6H_5), 3.53 (2 H, dd, $^2J_{P,H}$ 12.0, $^2J_{H,H}$ 14.0, H_a of CH_2Ph), 3.45 (2 H, dd, $^2J_{P,H}$ 14.0, $^2J_{H,H}$ 14.0, H_b of CH_2Ph), 0.792 (3 H, s, sat, $^2J_{Hg,H}$ 191.6, CH_3). ^{13}C NMR (CD_2Cl_2, *J*/Hz): δ 7.1[*J*(Cα,^{31}P) 1441], 14.1[*J*(Cβ-^{31}P) 43.0], 36.7[*J*(C_0-^{31}P) 64.0], 131.0, 130.5, 129.0, 127.5[*J*(C_n-^{31}P) 8.7, 5.2, 2.8, 3.2], 250.3 [*J*(C_7-^{31}P) 54.8].

[$PhHg\{S_2CP(O)(CH_2Ph)_2\}$] (8). K[L2] (1.13 g, 3.28 mmol) and HgPhCl (1.11 g, 3.54 mmol) were filled in a Schlenk flask under N_2, 20 mL methanol added and the suspension stirred for 10 min. The solution gradually turned wine-red and a pink precipitate started to form. The product was filtered off, washed with methanol and dried in *vacuo*. Yield: 1.4 g, 73%, pink powder. Calc. for $C_{21}H_{19}OPS_2Hg$: C, 43.3; H, 3.28. Found: C, 42.2; H, 3.23. M.p.: 165–167 °C (dec.). IR (KBr, cm^{-1}): 1175 (s) [$\tilde{\nu}$(P=O)], 1055 (s) and 918 (m) [$\tilde{\nu}$(CS_2)]. UV–vis (CH_2Cl_2, λ/nm, ε/$M^{-1}\cdot cm^{-1}$): λ 549 (n to π*, logε 1.52), 358 (π to π*, logε 3.87). ^{1}H NMR (CD_2Cl_2, *J*/Hz): δ 7.3–7.2 (10 H, m, C_6H_5-P), 7.3–7.5(5 H, m, C_6H_5-Hg, $^3J_{Hg,Ho}$ 179), 3.56 (2 H, dd, $^2J_{P,H}$ 12.0, $^2J_{H,H}$ 14.1, H_a of CH_2Ph), 3.45 (2 H, dd, $^2J_{P,H}$ 14.0, $^2J_{H,H}$ 14.1, H_b of CH_2Ph). ^{13}C NMR (CD_2Cl_2, *J*/Hz): δ 155.8[*J*($C_{i,\pi\sigma o}$,^{31}P) 2233], 137.6, 129.1, 128.8[*J*($C_{o,\mu,\pi}$-^{31}P) 110.6, 189, 33], 36.7[*J*(C_0-^{31}P) 64.3], 131.0, 130.5, 129.0, 127.5[*J*(C_n-^{31}P) 8.7, 5.2, 2.8, 3.2], 249.9 [*J*(C_7-^{31}P) 54.3].

X-ray Crystallography: Crystal data for **1** were collected by using an Agilent Technologies SuperNova A diffractometer fitted with an Atlas detector using Mo-K_α radiation (0.71073 Å). A complete dataset was collected, assuming that the Friedel pairs are not equivalent. An analytical numeric absorption correction was performed [36]. The structure was solved by direct methods using SHELXS-97[37] and refined by full-matrix least-squares fitting on F^2 for all data using SHELXL-97 [37]. Hydrogen atoms were added at calculated positions and refined by using a riding model. Their isotropic temperature factors were fixed to 1.2 times (1.5 times for methyl groups) the equivalent isotropic displacement parameters of the carbon atom the H-atom is attached to. Anisotropic thermal displacement parameters were used for all non hydrogen atoms. CCDC-1037541 contains the supplementary crystallographic data for this paper. These data can be obtained free of charge from The Cambridge Crystallographic Data Center via www.ccdc.cam.ac.uk/data_request/cif.

Crystal data for **6′** is provided in the supplementary section where the data refinement was not completed due to deterioration of the crystal. The data was collected on an Enraf-Nonius CAD4 diffractometer equipped with an Oxford Cryostreams low-temperature device. Data reduction was performed with the DREADD program package 20 and absorption correction with the ABSORB set of programs [38]. The structures were solved by direct methods using SHELXS [39] and completed by subsequent Fourier difference synthesis and refined with SHELXL. All hydrogen atoms were placed at idealized positions. The isotropic displacement parameters for all the hydrogen atoms were constrained to be 1.2 times the equivalent isotropic displacement parameter of the atom to which a hydrogen atom is covalently bonded [38,39].

Acknowledgements

Thanks are extended to Dr. Helge Mueller-Bunz, at University College Dublin, Dublin, Ireland and to Professor Martin Albrecht, University of Bern, Bern, Switzerland, for crystal data collection and structure finalizing. The authors also thank MA for insightful discussion. Mr. Dmitrii Razinkov and Ms. Hafdís I. Ingvarsdottir are thanked for help with sample preparation for solution IR measurements. Financial support from the Science Institute, Chemistry Department, is gratefully acknowledged.

Appendix A. Supplementary data

Crystallographic details for compound **1** are included in Table SI1 and in cif format. Bond lengths and angles for **6′** are included in Table SI2.

Supplementary data related to this article can be found at https://doi.org/10.1016/j.jorganchem.2017.11.002.

References

[1] (a) D. Coucouvanis, Prog. Inorg.Chem. 11 (1970) 233–371;
(b) D. Coucouvanis, Prog. Inorg. Chem. 26 (1979) 301–469;
(c) R. Eisenberg, Prog. Inorg. Chem. 12 (1970) 295–369.
[2] G. Gattow, W. Behrendt, Topics in Sulfur Chemistry 2, Georg Thieme Publishers, Stuttgart, Germany, 1977.
[3] C. Silvestru, J.E. Drake, Coord. Chem. Rev. 223 (2001) 117–216.
[4] (a) R. Kramolowsky, Angew. Chem. 81 (1969) 182–183;
(b) O. O Dahl, N.C. Gelting, O. Larsen, Acta Chem. Scand. 23 (1969) 3369–3375;
(c) O. Dahl, Acta Chem. Scand. 25 (1971) 3163–3171;
(d) J. Kopf, R. Lenck, S.N. Olafsson, R. Kramolowsky, Angew. Chem. 88 (1976) 811–812;
(e) A.W. Gal, J.W. Gosselink, F.A. Vollenbroek, J. Organomet. Chem. 142 (1977) 357–374;
(f) F.G. Moers, D.H.M.W. Thewissen, J.J. Steggerda, J. Inorg. Nucl. Chem. 39 (1977) 1321–1322.
[5] (a) U. Kunze, A. Antoniadis, J. Organomet. Chem. 215 (1981) 187–200;
(b) K.G. Steinhauser, W. Klein, R. Kramolowsky, J. Organomet. Chem. 209 (1981) 355–372;
(c) D. Dakternieks, B.F. Hoskins, E.R.T. Tiekink, Aust. J. Chem. 37 (1984) 197–203.
[6] (a) E. Hey, M.F. Lappert, J.L. Atwood, S.G. Bott, J. Chem. Soc. Chem. Commun. (1987) 421–422;
(b) E.M. Váques-Lópes, A. Sánchez, J.S. Casas, J. Sordo, E.E. Castallano, J. Organomet. Chem. 438 (1992) 29–37;
(c) K.-H. Yih, Y.-C. Lin, M.-C. Cheng, Y. Wang, J. Chem. Soc. Dalton Trans. (1995) 1305–1313.
[7] (a) P. Colamarino, P.L. Orioli, W.D. Benzinger, H.D. Gillman, Inorg. Chem. 15 (1976) 800–804;
(b) V. Chandrasekhar, A. Chandrasekaran, R.O. Day, H.M. Holmes, R.R. Holmes, Phosphorus, Sulfur Silicon 115 (1996) 125–139.
[8] J.S. Casas, A. Castineiras, I. Haiduc, A. Sanchez, J. Sordo, E.M. Vazquez-Lopez, Polyhedron 13 (1994) 2873–2879.
[9] V. Garcia-Montalvo, J. Novosad, P. Kilian, J.D. Woollins, A.M.Z. Slawin, P. Garcia y Garcia, M. Lopez-Cardoso, G. Espinosa-Perez, R. Cea-Olivares, J. Chem. Soc. Dalton Trans. (1997) 1025–1030.
[10] (a) R.A. Varga, J.E. Drake, C. Silvestru, J. Organomet. Chem. 675 (2003) 48–56;
(b) R.A. Varga, J.E. Drake, C. Silvestru, Phosphorus, Sulfur Silicon 169 (2001) 47–50.
[11] S.N. Ólafsson, T.N. Petersen, P. Andersen, Acta Chem. Scand. 50 (1996) 745–748.
[12] V. Garcia-Montalvo, R. Cea-Olivares, G. Espinosa-Perez, Polyhedron 15 (1996) 829–834.
[13] M.G. Begley, C. Gaffney, P.G. Harrison, A. Steel, J. Organomet. Chem. 289 (1985) 281–293.
[14] F.T. Edelmann, I. Haiduc, C. Silvestru, H.-G. Schmidt, M. Noltemeyer, Polyhedron 17 (1998) 2043–2047.
[15] A.-F. Shihada, F.Z. Weller, Anorg. Allg. Chem. 627 (2001) 638–644.
[16] S.N. Ólafsson, C. Flensburg, P. Andersen, J. Chem. Soc. Dalton Trans. (2000) 4360–4368.
[17] S.N. Ólafsson, R. Bjornsson, O. Helgason, S. Jonsdottir, S.G. Suman, J. Organomet. Chem. 825 (2016) 125–138.
[18] (a) N. Singh, A. Kumar, R. Prasad, K.C. Malloy, M.F. Mahon, Dalton Trans. 39 (2010) 2667–2675;
(b) V. Singh, R. Chauhan, A. Kumar, L. Bahadur, N. Singh, Dalton Trans. 39 (2010) 9779–9788;
[19] N. Singh, A. Kumar, K.C. Molloy, M.F. Mahon, Dalton Trans. (2008) 4999–5007.
[20] C. Silvestru, J. E. Drake, Coord. Chem. Rev.., 2001, 223, 117–216.
[21] (a) R. Rösler, J.E. Drake, C. Silvestru, J. Yang, I. Haiduc, J. Chem. Soc. Dalton Trans. (1996) 391–399;
(b) C. Silvestru, R. Rösler, A. Silvestru, J.E. Drake, J. Organomet.Chem. 642 (2002) 71–79.
[22] D.F. Fenske, R. Mattes, J. Löns, K.-F. Tebbe, Chem. Ber. 106 (1973) 1139–1144.
[23] G. Ruban, V. Zabel, Cryst. Struct. Comm. 5 (1976) 671–677.
[24] C. Chieh, L.P.C. Leung, Can. J. Chem. 54 (1976) 3077–3087.
[25] Y.S. Wong, A.J. Carty, P.C. Chieh, J. Chem. Soc. Dalton Trans. (1977) 1801–1808.
[26] J. Zukerman-Schpector, E.M. Vásquez-López, A. Sánchez, J.S. Casas, J. Sordo, J. Organomet.Chem 405 (1991) 67–74.
[27] (a) G. Rajput, M.K. Yadav, M.G.B. Drew, N. Singh, Dalton Trans. 44 (2015) 5909–5916;
(b) G. Rajput, M.K. Yadav, T.S. Thakur, M.G.B. Drew, N. Singh, Polyhedron 69 (2014) 225–233.
[28] R. Dulare, M.K. Bharty, S.K. Kushawaha, S. Singh, N.K. Singh, Polyhedron 30 (2011) 1960–1967.
[29] (a) J.L. Wardell, Organometallic Compounds of Zinc, Cadmium and Mercury, Chapman and Hall, 1985;
(b) A. Bondi, J. Phys. Chem. 68 (1964) 441–452.
[30] V. Singh, A. Kumar, R. Prasad, G. Rajput, M.G.B. Drew, N. Singh, Cryst. Eng. Comm. 13 (2011) 6817–6826.
[31] (a) M.J. Jansen, Recl. Trav. Chim. Pays-Bas 79 (1960) 450–463;
(b) M.L. Shankaranarayana, C.C. Patel, Acta Chem. Scand. 19 (1965) 1113–1119;
(c) J. Fabian, Theor. Chim. Acta 12 (1968) 200–205;
(d) G.S. Nikolov, N. Tyutyulkov, Inorg. Nucl. Chem. Lett. 7 (1971) 1209–1212.
[32] (a) C. Silvestru, A. Silvestru, I. Haiduc, R.G. Ramirez, R. Cea Olivares, Heteroat. Chem. 5 (1994) 327–336;
(b) D. De Vos, A.A. Barneveld, D.C. Van Beelen, J. Wolters, Recl. Trav. Chim. Pays-Bas 98 (1979) 202–208.
[33] J.S. Casas, E. Castellano, J. Ellena, I. Haiduc, A. Sánchez, R.F. Semeniuc, J. Sordo, Inorg. Chim. Acta 329 (2002) 71–78.
[34] H.J. Reich, WinDNMR: dynamic NMR spectra for windows, J. Chem. Educ. 72 (12) (1995) 1086. Software 3D2.
[35] S. N. Ólafsson, Ph.D. Thesis, University of Hamburg Germany, 1973.
[36] R.C. Clark, J.S. Reid, Acta Crystallogr. A51 (1995) 887–897.
[37] G.M. Sheldrick, Acta Crystallogr. A64 (2008) 112–122.
[38] G.T. De Titta, ABSORB, J. Appl. Crystallogr. 18 (1985) 75–79.
[39] G.M. Sheldrick, SHELXS 97: Program for Crystal Structure Analysis, Univ. Göttingen (1997).
[40] H. I. Ingvarsdottir, MS Thesis, University of Iceland, 2017.